Case Studies in Construction Materials 5 (2016) 64–78

Contents lists available at ScienceDirect

Case Studies in Construction Materials

journal homepage: www.elsevier.com/locate/cscm

Case study

Compressive strength capacity of light gauge steel composite columns

W. Leonardo Cortés-Puentes[a,*], Dan Palermo[b], Alaa Abdulridha[a], Muslim Majeed[a]

[a] Department of Civil Engineering, University of Ottawa, 161 Louis Pasteur St., Ottawa ON K1N 6N5, Canada
[b] Department of Civil Engineering, York University, 4700 Keele St., Toronto ON M3J 1P3, Canada

ARTICLE INFO

Article history:
Received 27 May 2016
Received in revised form 16 August 2016
Accepted 17 August 2016
Available online 19 August 2016

Keywords:
Composite columns
Light gauge steel
Compressive strength capacity
Full-scale testing

ABSTRACT

The axial compressive strength capacity of concrete-filled light gauge steel composite columns was assessed through an experimental program involving twelve long and fourteen stub columns with width-to-thickness ratio of 125 for the encasing steel section. A comparison between concrete-only and confined stub columns demonstrated that the stub column experiences an increase of strength of up to 16% due to confinement. The compressive strength contribution of the light gauge steel section was limited by local buckling. Specifically, the steel-only stub column sections lacking the concrete core experienced, on average, approximately 33% of its full compressive strength. The full-scale composite columns illustrated that the axial compressive strength capacity was controlled by end bearing capacity and local buckling of the light gauge steel. The axial compression strength capacity of the full-scale composite columns was satisfactorily predicted based on end bearing resistance of the concrete core and local strains in the light gauge steel. Furthermore, the 33% strength contribution established from the steel-only sections provided a satisfactory lower bound estimate for the calculation of axial compressive strength.

1. Introduction

Concrete-filled steel box columns are economical composite structural elements that are increasingly being used in the construction of industrial and high-rise office buildings. The composite action of concrete-filled steel columns provides a significant increase in stiffness, strength, and ductility relative to concrete-only or steel-only sections. The concrete core provides axial stiffness, compression strength, and enhances the buckling capacity of the encasing steel. The encasing steel provides confinement to the concrete and thus increases the axial strength and ductility. Typically, these systems consist of thick steel sections where local buckling is not a controlling performance criterion.

More recently, other construction materials have drawn the attention of the construction industry, such as concrete-filled light gauge steel box columns that are imbedded within the cavities of prefabricated modular walls and serve as gravity load resisting elements for low-rise buildings as illustrated in Fig. 1. Such a system provides stay-in-place formwork in addition to structural capacity for the columns. Furthermore, placing the columns within the cavities of modular walls provides open

* Corresponding author.
E-mail address: wcort032@uottawa.ca (W. L. Cortés-Puentes).

http://dx.doi.org/10.1016/j.cscm.2016.08.001

Fig. 1. Concrete-filled light gauge steel composite columns imbedded within prefabricated modular walls [1].

space within the building envelope. The axial compressive strength and confinement of composite columns is a function of the slenderness of the walls of the steel section. To simplify design, code provisions limit the width-to-thickness ratio to prevent local buckling prior to yielding. Light gauge cold formed steel composite columns, however, do not meet this requirement.

Several studies have investigated the response of concrete-filled tubular columns, specifically the effect of local buckling and confinement on the strength capacity. Most of these studies have been conducted on short columns encased within relatively thick hollow structural sections (HSS). Experimental testing has resulted in formulations prescribed by design standards, including: American ACI 318-14 [2], Japanese AIJ [3], Australian AS5100.6 [4], British BS5400-5 [5], Canadian CSA S16-14 [6], Chinese DBJ13-51 [7], and European Eurocode 4 [8]. Shakir-Khalil and Mouli [9], Schneider [10], and Sakino et al. [11] conducted experimental studies on square and rectangular composite columns to investigate the effect of column height, cross section and material properties on the axial strength and confinement of long and short concrete-filled steel columns with width-to-thickness ratios ranging from 15.5 to 73.8. The square and rectangular sections did not provide significant confinement to the concrete, and increasing the width-to-thickness resulted in limited post-yield response. Ge and Usami [12] investigated the effect of internal stiffeners on the local buckling capacity of concrete-filled steel box columns by testing short columns with width-to-thickness ratios between 43 and 73. The internal stiffeners affected the strength of the columns as a direct result of improved buckling response of the encasing steel. The improvement, however, was marginal for stiffeners with low rigidity. Yang and Han [13] investigated the effect of partial loading on circular and square concrete-filled steel sections with width-to-thickness ratio of 50. It was observed that under partial concentric compressive loading, the composite columns had reasonable bearing capacity and ductility. Other column shapes and materials have also been studied. Ren et al. [14] conducted tests on composite stub columns with non-typical rectangular or circular sections, and Zhou and Young [15] conducted tests on composite columns with encasing aluminum tubes.

In addition to experimental research, numerical modelling has been used to investigate the response of concrete-filled steel sections. Schneider [10] conducted numerical analyses to study the effect of width-to-thickness ratio on confinement. El-Tawil and Deierlein [16], and Lakshmi and Shanmugan [17] predicted the nonlinear response of concrete-filled steel columns analytically without the local buckling effect. Uy [18] investigated the effect of local buckling on the response of composite beams and short columns with maximum width-to-thickness ratio of 100. This study demonstrated that the axial strength capacity was limited by the contribution of the steel, which was based on the effective width method, and that local buckling had a significant effect on the response of the composite sections. Liang and Uy [19], and Liang et al. [20] used the nonlinear fibre element method to predict the response of concrete-filled box columns that were affected by local buckling of the encasing steel. An expression was developed to predict the stress-strain response and ultimate strength based on the effective width method. Chen et al. [21] investigated the effect of local buckling and concrete confinement of concrete-filled box columns under axial load by testing and numerically simulating a series of stub columns. Tao et al. [22] and Thai et al. [23] used the finite element method to predict the response of composite concrete-filled steel columns for a wide range of width-to-thickness ratios and material strengths. The finite element method has further been used to assess elliptical stainless steel stub sections filled with concrete [24]. Both strength and ductility of the concrete section were improved due to the elliptical encasing steel.

In general, studies on concrete-steel composite columns have focused on sections fabricated from thick, hot-rolled, steel with maximum width-to-thickness ratio of 100. To the best of the author's knowledge, concrete-filled composite columns incorporating light gauge steel sections with large width-to-thickness ratios have not been investigated. Limited studies incorporating thin encasing composite columns have focused on cold-formed steel sections. Ferhoune [25], Ferhoune and Zeghiche [26], Ellobody and Young [27], and Lam and Gardner [28] conducted tests on composite columns consisting of cold-formed steel sections with thicknesses ranging from 2 mm to 6 mm and width-to-thickness ratios of up to 50.

The literature clearly demonstrates that the axial strength capacity of concrete-filled composite sections is increased by the presence of the encasing steel. The strength contribution of the encasing steel, however, is significantly affected by buckling. Furthermore, the effect of confinement is negligible for square and rectangular composite columns with compact encasing steel sections when the concrete core and encasing steel are loaded simultaneously [10] and [21]. Although some degree of confinement has been observed in stub columns, studies have demonstrated that the contribution from steel sections to confinement of slender columns is negligible [29]. Extending these conclusions to light gauge encasing sections requires corroboration with experimental data. In addition, the lack of design procedures for structural engineers, and test data to corroborate new approaches, limits the design of light gauge composite systems. Therefore, the main objective of this study was to investigate the contributions of the various components of light gauge steel composite columns to the axial load strength capacity.

2. Design codes

There are no design standards that provide guidance to determine the axial compressive strength capacity of rectangular and square light gauge steel composite columns. Existing standards are applicable to stiff steel sections that are intended to prevent local instability of typical composite concrete-filled tubular columns. Most code provisions (ACI 318-14, AIJ, AS5100.6, BS5400-5, CSA S16-14, and Eurocode 4) prescribe formulations that specify the nominal compressive strength (not including global buckling), N_n, as the sum of the individual contributions of concrete core, N_c, and encasing steel, N_s (Eq. (1)); the exception being standard DBJ13-51, which combines the concrete and steel contributions into a single term (Eq. (2)). ACI 318-14 and CSA S16-14 limit the compressive capacity of the concrete core (Eq. (3)) to reflect the strength of concrete loaded as a column.

$$N_n = N_s + N_c = A_s f_y + A_c f_c \ (\text{AIJ},\ \ \text{AS5100.6}\ \ \text{BS5400} - 5, \text{and Euro code 4}) \tag{1}$$

$$N_n = N_{sc} = A_{sc} f_{sc};\quad f_{sc} = (1.18 + 0.85 z_o)\, f_c;\quad z_o = A_s f_y / A_c f_c \quad (\text{DBJ13} - 51) \tag{2}$$

$$N_n = \ N_s + \alpha_1 N_c = A_s f_y + \alpha_1 A_c f_c \quad (\text{ACI}\, 318 - 14 \text{ and } \text{CSA}\ \ \text{S16} - 14) \tag{3}$$

Where A_s and A_c are the encasing steel and concrete core cross sectional areas, respectively; A_{sc} is the total area of the composite section $(A_s + A_c)$; f_y is the yield stress of the steel; f_c is the characteristic concrete strength; z_o is a design constraining factor, and α_1 is a stress limit factor. Note that α_1 is 0.85 for ACI 318-14, and it is calculated as $\alpha_1 = 0.85 -$

None of the code provisions account for the effect of confinement for square and rectangular composite columns. Code provisions typically recognize the effect of confinement only for circular columns. To avoid reduction of stiffness and, therefore, reduction of axial strength capacity due to local buckling, code provisions limit the width-to-thickness ratio (b/t) of both sides of square and rectangular columns according to the limits provided in Table 1.

3. Experimental program: light gauge steel composite stub columns

Two types of 1.22 mm-thick, 18 gauge steel sections were used in this study, referred to as Profile A and Profile B (Fig. 2). The difference between the two profiles is the cross section shape near the lock seams. The intent of the lock seams is to provide sections that can easily slide into each other to form a tubular section, which eliminates welding. Fourteen, 152 mm × 152 mm × 305 mm, stub columns (referred to as SB) were tested to better understand the behaviour of light gauge steel composite columns subjected to compression loading.

Table 1
Width-to-thickness limits for square and rectangular composite columns.

Code	Width-to-Thickness Limit
ACI 318-11	$\frac{b}{t} \le \sqrt{\frac{3E_s}{f_y}}$
AIJ	$\frac{b}{t} \le 1.5\frac{734}{\sqrt{f_y}}$
AS5100.6	$\frac{b}{t} \le 52\sqrt{\frac{235}{f_y}}$
BS5400-5	$\frac{b}{t} \le \sqrt{\frac{3E_s}{f_y}}$
CSA S16-01	$\frac{b}{t} \le \frac{1350}{\sqrt{f_y}}$
DIBJ13-51	$\frac{b}{t} \le 60\sqrt{\frac{235}{f_y}}$
Eurocode 4	$\frac{b}{t} \le 52\sqrt{\frac{235}{f_y}}$

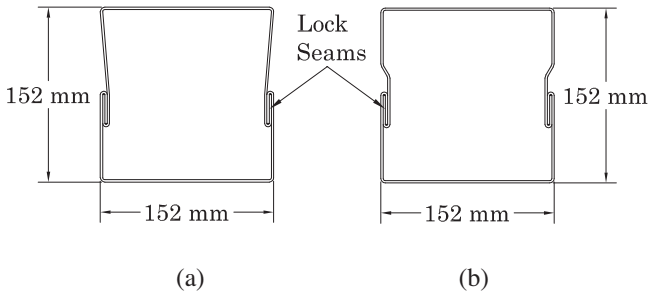

Fig. 2. Cross section of encasing light gauge steel: (a) Profile A; and (b) Profile B.

Four sets of columns were tested (Fig. 3): concrete-only (SB-CON), steel-only (SB-STL), confinement (SB-CUT), and composite (SB-COM). Three concrete-only columns were constructed using the light gauge steel encasing section as a mould, which was removed after the concrete was cured. Four steel-only columns consisted of the steel encasing section without a concrete core. Four confinement columns included both the concrete core and light gauge steel section; however, a 25 mm section of the encasing steel was removed at the top and bottom of the columns to avoid contribution from the steel to the axial compressive strength capacity. Three composite columns were built with the light gauge steel sections encasing a concrete core. Columns SB-CON and SB-STL were tested to determine the individual contributions of the concrete and light gauge steel, respectively; while Columns SB-CUT were intended to assess the effect of confinement. Composite Columns SB-COM were tested to study the response of the composite section. Profile B was used in the constructing of the stub columns (Fig. 3(a)). [Both Profiles A and B were used for the full-scale long columns.] The cross section of the stub columns was full-scale and similar to that being proposed for the construction industry (Fig. 1). Table 2 provides details of the geometry and the materials used for the construction of the stub columns. Note that the steel properties were obtained from coupon tests, while the concrete properties were obtained from cylinder tests on the day of testing.

Loading was imposed with a 2200 kN capacity compression testing machine (Fig. 4(a)). Loads were recorded with a built-in load cell and axial displacements were recorded with two Linear Variable Displacement Transducers (LVDTs) placed on two opposite sides of the columns as shown in Fig. 4(a). Longitudinal and transverse strains of the steel section at mid-height

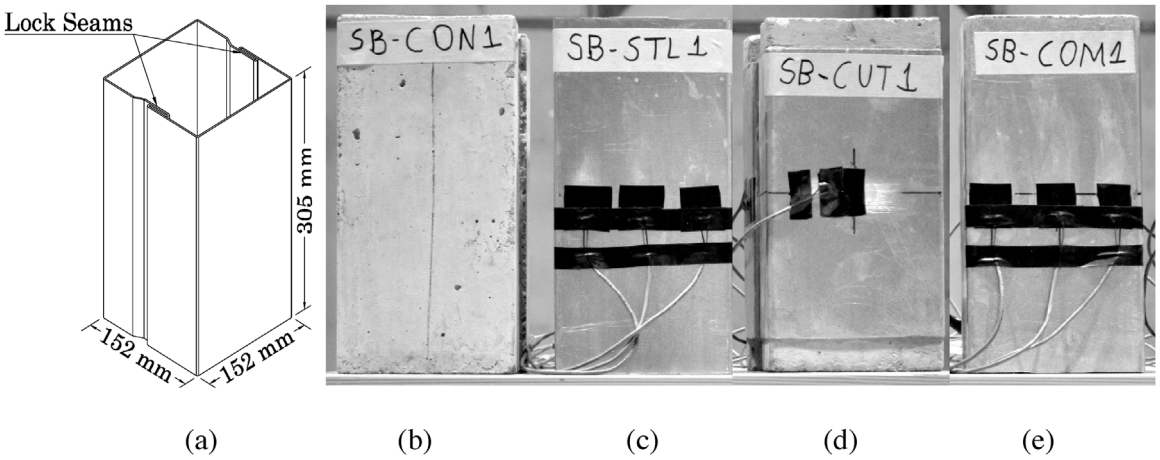

Fig. 3. Stub columns: (a) steel section; (b) concrete-only columns; (c) steel-only columns; (d) composite columns; and (e) confinement columns.

Table 2
Details of stub columns.

Column	Cross-Section	Length	Concrete Core	Encasing Steel	
	(mm × mm)	(mm)	f'_c (MPa)	f_y (MPa)	E_s (MPa)
SB-CON	152 × 152	305	24.1	–	–
SB-STL	152 × 152	305	–	429	204,000
SB-CUT	152 × 152	305	24.1	429	204,000
SB-COM	152 × 152	305	24.1	429	204,000

Note: f'_c = cylinder compressive strength; f_y = yield strength; and E_s = modulus of elasticity

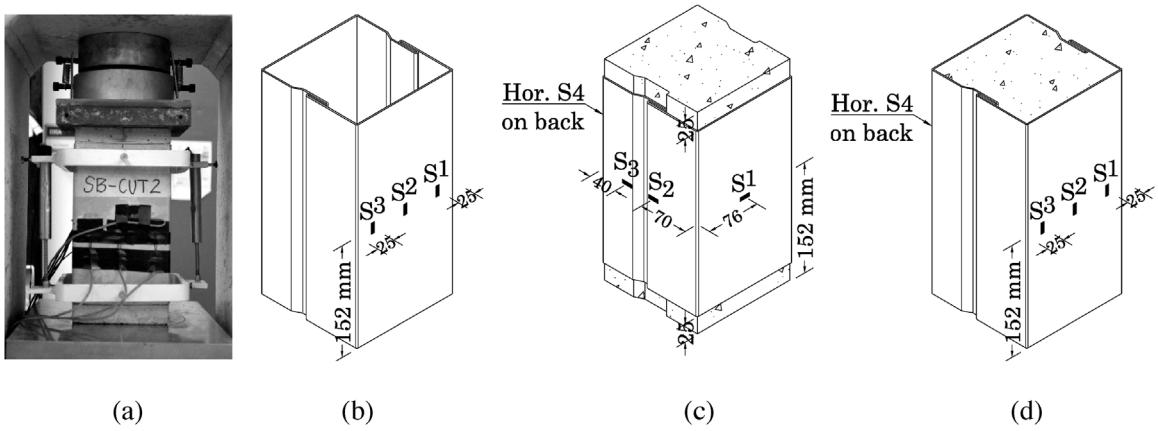

Fig. 4. Instrumentation on stub columns: (a) test setup and LVDTs; (b) strain gauges on steel-only columns (SB-STL); (c) strain gauges on confinement columns (SB-CUT); and (d) strain gauges on composite columns (SB-COM).

of Columns SB-STL, SB-CUT, and SB-COM were captured with 10 mm strain gauges as illustrated in Fig. 4(b), (c), and (d), respectively. Table 3 provides the axial strength capacity recorded for each set of columns. Typical failures of the concrete-only, steel-only, confinement, and composite columns are provided in Fig. 5.

3.1. Concrete-only stub columns

Three, concrete-only stub columns with cross sectional area of 22,088 mm^2, and two, 100 mm diameter $\times$ 200 mm high, standard concrete cylinders with cross sectional area of 7854 mm^2 were tested to determine the concrete contribution. The compressive strengths for the two cylinders were 23.05 MPa and 25.11 MPa, and the corresponding standard deviation was 1.46 MPa. The characteristic concrete compressive strength of 24.1 MPa for the stub columns was based on the average strength of the two concrete cylinders.

The axial load-strain responses of the concrete-only stub columns are provided in Fig. 6. [The strains were determined from the displacements recorded by the LVDTs.] Column SB-CON3 provided the most representative compressive behaviour of the specimens (similar to the response of the cylinders), while Columns SB-CON1 and SB-CON2 displayed uncharacteristic post-peak responses. Column SB-CON1 experienced a sudden drop of strength after reaching the peak strength, and Column SB-CON2 exhibited an atypical plateau for unconfined concrete. Anomalies in Columns SB-CON1 and SB-CON2 were attributed to crushing of the concrete at the top and bottom, which affected the post-peak behaviour. The average peak load for the concrete-only stub columns was 558 kN (Table 3) corresponding to a compressive stress of 25.3 MPa; approximately

Table 3
Recorded axial compressive strength of stub columns.

Column	Strength [kN]		COV [%]
	Peak	Average	
SB-CON1	546	558	8.2
SB-CON2	519		
SB-CON3	608		
SB-STL1	130	127	5.3
SB-STL2	133		
SB-STL3	118		
SB-STL4	126		
SB-CUT1	657	649	5.4
SB-CUT2	598		
SB-CUT3	679		
SB-CUT4	662		
SB-COM1	727	762	4.1%
SB-COM2	775		
SB-COM3	785		

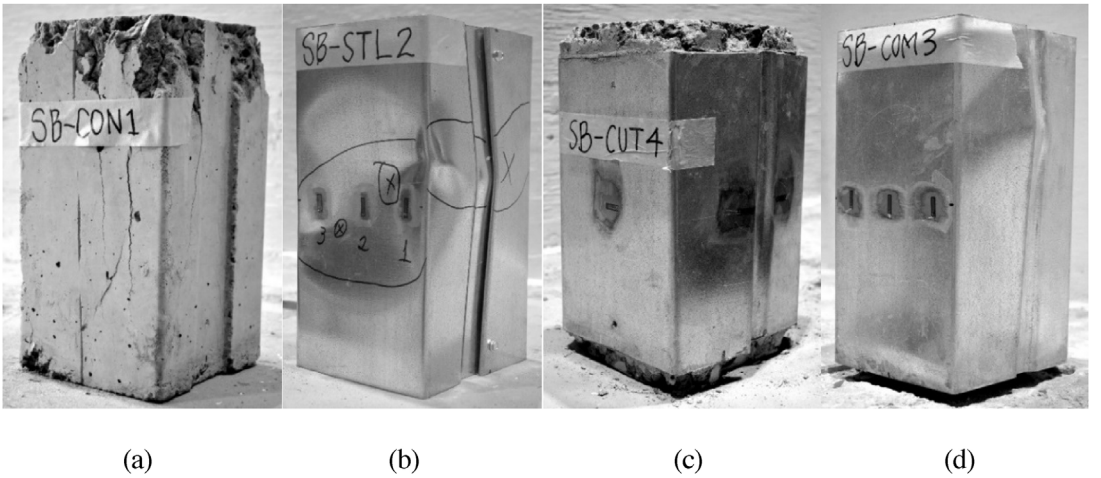

Fig. 5. Typical damage of stub columns: (a) concrete-only; (b) steel-only; (c) confinement; and (d) composite.

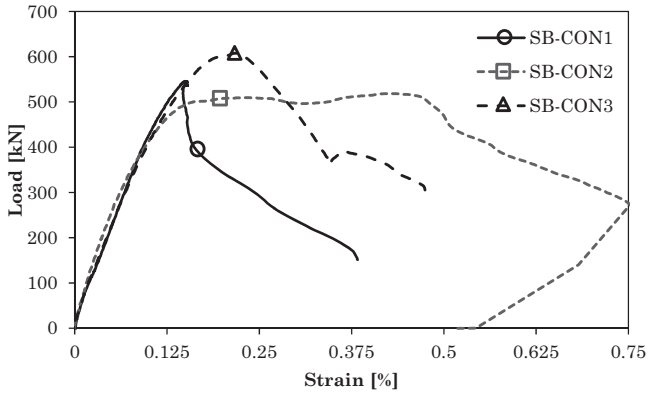

Fig. 6. Axial load-strain response of concrete-only columns SB-CON.

5% greater than that of the cylinders. In general, concrete circular cross sections provide reduced compressive strength relative to square cross sections. Typical failure in the form of crushing of concrete was observed for the concrete-only stub columns (Fig. 5(a)).

The testing of the concrete cylinders and concrete core of the stub columns suggests that the cylinder compressive strength, f'_c, is conservative and adequate for calculating the concrete core contribution to the axial strength capacity of the light gauge steel composite columns.

3.2. Steel-only stub columns

Four, steel-only stub columns with cross sectional area of 906 mm^2 were tested to assess the contribution of the steel section. The global axial load-strain responses for Columns SB-STL2, SB-STL3, and SB-STL4 are provided in Fig. 7, while the peak strength only was recorded for Column SB-STL1 (straight line in Fig. 7). The LVDTs slipped during testing of SB-STL1; therefore, the axial displacements of the column were not captured. [The global strains were calculated from the displacements recorded by the LVDTs (Fig. 4(a)).] The average peak compressive strength was 127 kN (Table 3) corresponding to average peak stress of 140 MPa.

Three longitudinal strain gauges: S1, S2, and S3 (Fig. 4(b)) recorded the local strain distribution. Strain Gauge S2 was located at the centre of the section, and Strain Gauges S1 and S3 were located 25 mm from the edges, approximately half of the post-local buckling effective width of the section. The effective width was established following CSA S136-12 [30] for stiffened cold-formed steel members supported by a web on each longitudinal edge. Based on the properties of the light gauge steel (f_y = 429 MPa, b/t = 125, ν = 0.3, and E = 204 GPa), the effective width of the section was calculated to be 47 mm. [The effective width method assumes that maximum compressive stresses (critical local buckling stresses) are uniformly distributed near the edges of the section, while zero compressive stresses are assumed at the centre of the width.]

The local longitudinal strains and, therefore, corresponding stresses of the steel sections were scattered as demonstrated by the strains recorded by Strain Gauge S2 at the centre of the sections (Fig. 8). Similar scatter was recorded by Strain Gauges S1 and S3 near the edges. The scatter resulted in various peak stress profiles on the front side of the sections, as illustrated in Fig. 9. Note that the stresses in Fig. 9 were calculated from the peak strains.

The steel-only columns experienced various modes of local buckling at mid-height and at the ends (Fig. 5(b)). The strains and corresponding stresses on the front face were influenced by the buckling pattern and the axial and bending stiffness of the adjacent perpendicular edge faces. The strain gauges captured localized axial and bending strains, and therefore stresses, on the outside surface of the steel section, which differed from the global strains (and stresses) of the columns (Fig. 7). The post-buckling deformations of the columns are illustrated in Fig. 9. Larger strains (and stresses) were recorded for the columns that experienced larger buckling deformations. Due to the influence of local effects and scatter of the local axial

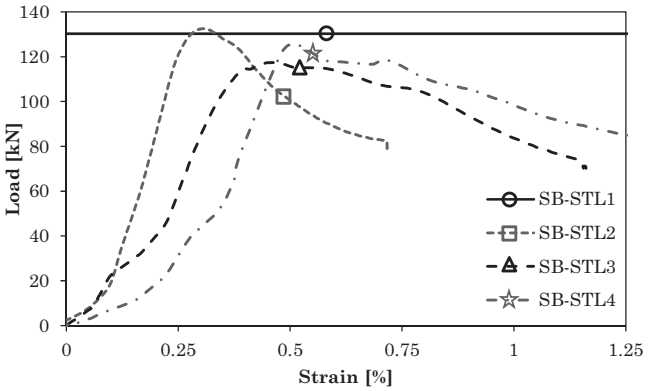

Fig. 7. Axial load-strain response of steel-only columns SB-STL.

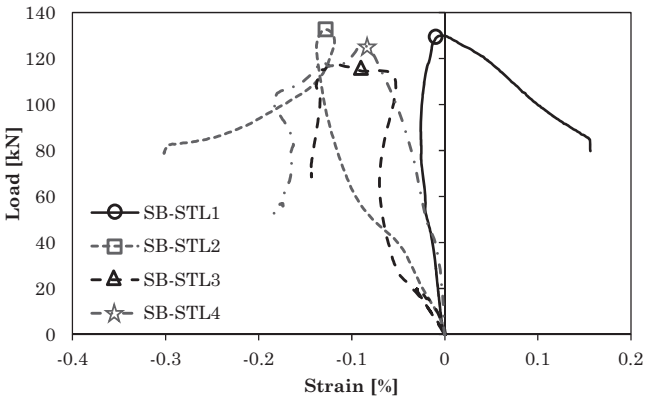

Fig. 8. Average longitudinal strain on steel section at mid-height of steel-only columns.

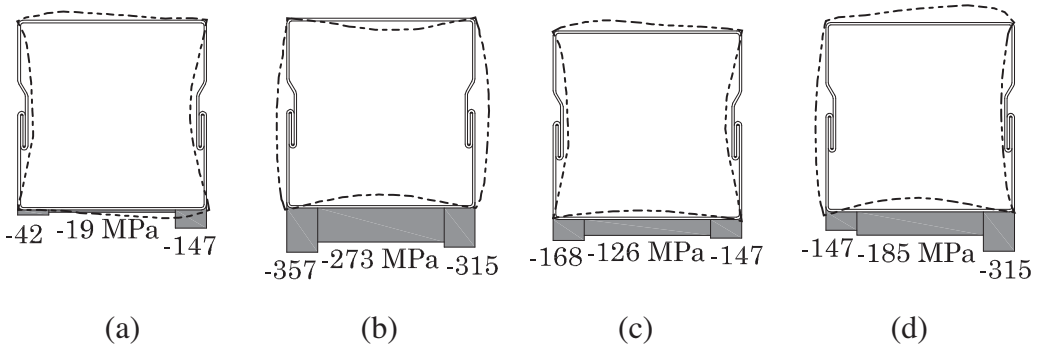

Fig. 9. Stress distribution and post-buckling deformation (dashed lines) at mid-height of steel-only columns: (a) SB-STL1; (b) SB-STL2; (c) SB-STL3; and (d) SB-STL4.

strains, the calculated stresses at mid-height were not consistent and did not provide a reliable compressive stress capacity for the light gauge steel sections. Therefore, the axial strength capacity of the encasing light gauge steel section should be based on the global results provided by the load cells.

The average yield stress and modulus of elasticity from tensile coupon testing of the light gauge steel were 429 MPa and 204,000 MPa, respectively; while average peak stress, based on the readings from the load cell, of 140 MPa and modulus of elasticity of approximately 75,000 MPa were recorded for the steel-only stub columns. Thus, the steel-only columns provided approximately 33% of the coupon strength and 37% of the coupon stiffness. The reduction in strength was due to substantial plastic local buckling at several locations which initiated approximately at the peak load. A probable cause of the reduction of stiffness was local elastic buckling throughout the column.

Although the behaviour of the steel-only columns are expected to differ from the response of the steel section in the composite columns, the global results recorded by the load cells were assumed to provide a lower bound for the contribution of the light gauge steel to the strength capacity. Other studies [31] have demonstrated that square composite concrete-filled steel sections subjected to axial loading sustain higher strength than the individual combinations of the steel section and the concrete core. This is attributed to the restraining effect that the concrete core has on the steel section, which, in turn, enhances the strength of the composite section.

3.3. Confinement stub columns

The effect of confinement was investigated by testing four stub columns: SB-CUT1, SB-CUT2, SB-CUT3, and SB-CUT4. The intent was to determine the level of confinement provided by the light gauge steel section if no axial load is transferred to the section. The global load-strain response of Column SB-CUT1 was satisfactorily captured (Fig. 10) and characterized by a typical parabolic behaviour where the post-peak branch experienced marginal softening. Sliding of the encasing steel section and concrete softening at the top and bottom of the columns prevented the global load-strain response of Columns SB-CUT2, SB-CUT3, and SB-CUT4 from being properly recorded. The peak strength for these columns, however, was satisfactorily recorded (Table 3) and represented with straight lines in Fig. 10. [The global strain was established from the displacements recorded by the LVDTs.] The average peak strength of 649 kN for the confinement columns was 91 kN greater than the strength recorded for the concrete-only columns. Therefore, the confining effect of the light gauge encasing steel section increased the column strength by approximately 16%.

Four strain gauges were placed in the horizontal position on the steel section at mid-height of the columns to measure local lateral strains (Fig. 4(c)), with the exception of Column SB-CUT1, where only two strain gauges were used.

The local lateral strain responses of the front face of the columns, recorded by Strain Gauge S1, are provided in Fig. 11(a). Similar response was recorded on the back face with Strain Gauge S4. The change from tensile to compressive straining at approximately 250 kN for some columns arose due to the effect of the expansion and opening of the steel section on the faces with the lock seams. These strains returned to the tensile regime near the peak load. The confinement columns experienced an average peak lateral strain of 0.009% on the front face. The lateral strain responses for the side of the columns, measured with Strain Gauge S3, are shown in Fig. 11(b). In general, compressive strains were recorded and the average peak lateral compressive strain was 0.038%. Lateral expansion of the concrete pushed the steel section outward, forcing the lock seams to open and the front and back faces without lock seams to stretch and bend. Opening of the section induced tensile strains on the front and back faces (Fig. 11(a)) and compressive strains on the side faces (Fig. 11(b)). The confinement mechanism is illustrated in Fig. 12.

Lateral stresses calculated on the light gauge steel section from the strain gauge data were not uniform. Therefore, a representative value for strength estimate was not established from the lateral strains. However, results from the confinement columns indicate that for the 152 mm × 152 mm composite sections, the strength of concrete is increased by

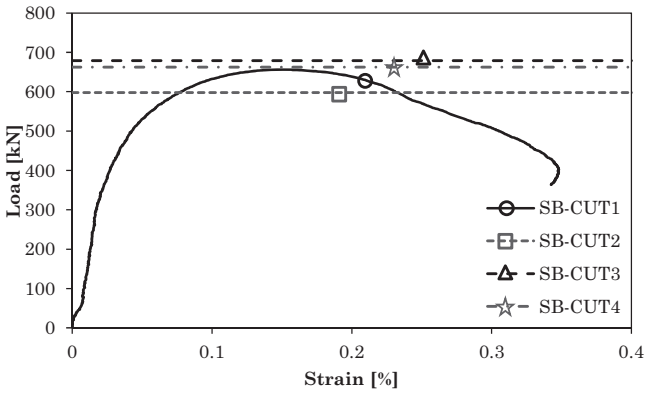

Fig. 10. Axial load-strain response of confinement columns SB-CUT.

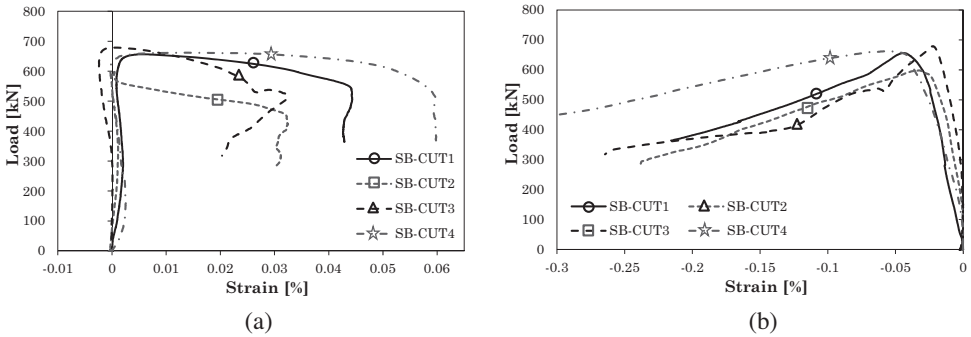

Fig. 11. Average lateral strain on steel section at mid-height of confinement columns: (a) front face; and (b) side faces.

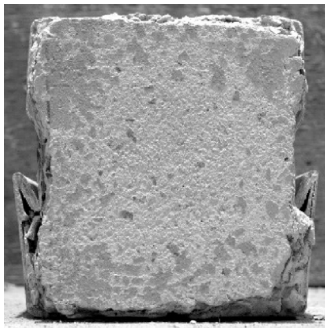

Fig. 12. Expansion of concrete and opening of steel section.

approximately 16% when confined with 1.22 mm thick light gauge sections with side lock seams where no axial load is transferred to the steel section.

3.4. Composite stub columns

Three stub columns were tested to record the axial compressive strength capacity of light gauge steel composite columns. The global axial load-strain responses for Composite Columns SB-COM are illustrated in Fig. 13. The average peak strength was 762 kN (Table 3). The strain corresponding to peak strength was similar for Columns SB-COM1 and SB-COM2 (approximately 0.10%), but significantly larger for Column SB-COM3 (approximately 0.24%). The axial deformations in SB-COM1 and SB-COM2 were measured over the 200 mm central part of the columns, while the deformations in Column SB-COM3 were measured along the entire height of the column (305 mm). The former did not capture the concrete softening deformations at the top and bottom of the columns.

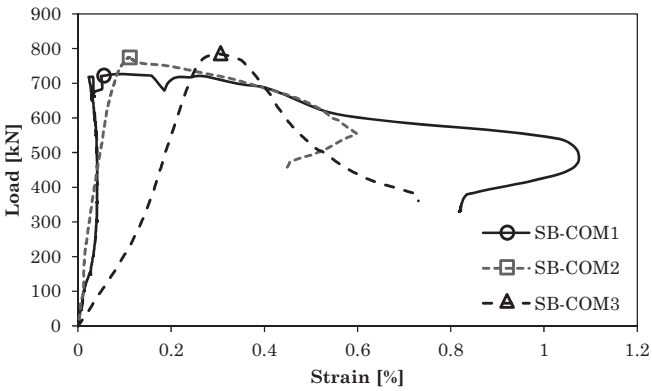

Fig. 13. Axial load-strain response of composite columns SB-COM.

The average peak local longitudinal compressive strain, measured by Strain Gauges S1, S2, and S3 at mid-width, was 0.046% (Fig. 14(a)). This average strain was, in general, smaller than the vertical strains observed on the steel-only columns, specifically those for Columns SB-STL2, SB-STL3, and SB-STL4, where larger inward buckling deformations at mid-height was observed. The smaller longitudinal strains along with less buckling demonstrated the beneficial effect of the concrete core. The average lateral strain measure by Strain Gauge S4 was 0.031% at peak load (Fig. 14(b)). This was similar in magnitude to that measured for the confinement columns SB-CUT (Fig. 11(b)). However, the lateral strains measured on the confinement columns were compressive due to the influence of the lock seams and the lack of axial loading on the steel section.

Based on the limited stub column tests, the sum of the average strengths of the steel-only stub columns and confinement stub columns of 776 kN was in close agreement (1.8% greater) with the average axial compressive strength of 762 kN of the composite columns. Furthermore, the sum of the averages of the concrete-only stub columns and steel-only stub columns of 685 kN was 77 kN (10%) lower than the average axial compressive strength of the composite columns. These comparisons suggest that for stub columns, the axial compressive strength capacity has contributions from the core concrete, light gauge steel section, and the effect of confinement. However, the effect of confinement decreases when the load is simultaneously applied to both the concrete core and the steel section. Ignoring the confinement effect provides a reasonable conservative estimate of the axial load capacity. An improved estimate of the axial load capacity would require better understanding of the restraining effect of the concrete core on the light gauge steel section. This phenomenon affects both the axial contribution of the steel section and apparent confinement effect of the steel section on the concrete core. Further experimental testing is required to assess this effect.

4. Experimental program: light gauge steel composite full-scale columns

Twelve, full-scale light gauge steel composite columns were tested. The columns were named according to the depth, the confinement profile, and the length. In general, the specimens were named C#1-X#2. The letter C denotes “Column”, the number #1 denotes the cross section depth in inches, the letter X denotes the light gauge steel profile, and the number #2 refers to the member length in feet. The columns were either 8 ft (2440 mm) or 9 ft (2745 mm) in length. All columns had the same width of 6 in (152 mm) and three different depths: 6 in (152 mm), 12 in (305 mm), and 18 in (457 mm). The corresponding length-to-width ratios (l/b) for the 8 ft and 9 ft columns were 16.1 and 18.1, respectively, and the slenderness ratios (kl/r) were 55.5 and 62.5, respectively. The columns were constructed from single, 152 mm × 152 mm, units with the same cross section as those of the stub columns (Fig. 15). Therefore, the 305 mm × 152 mm, and 457 mm × 152 mm columns were fabricated from 2 and 3 units, respectively. All the columns were reinforced with one 20 M reinforcing bar (19.5 mm diameter and 200 mm^2 area) positioned at the centre of each 152 mm × 152 mm unit. For Profile A column units, the concrete core and light gauge steel had cross sectional areas of 21,721 mm^2 and 903 mm^2, respectively. For Profile B column units, the cross sectional area of the core concrete and light gauge steel were 22,088 mm^2 and 906 mm^2, respectively. Note that the two columns lengths and various combinations of single units represent the different full scale applications in the field. Table 4 provides details of the geometry and the materials used for the construction of the long columns.

The test setup consisted of a concentric axial loading system using displacement-controlled actuators positioned between reactions frame and a loading beam (Fig. 16(a)). Two actuators were used for Columns C6 and C12 (Fig. 16(b)), while three actuators were used for Columns C18 (Fig. 16(c)). The reaction frames consisted of three stiff steel A-frames, while the loading beam consisted of a 610 mm × 610 mm built-up steel box section. The columns were simply supported at the ends (pinned supports) by steel plates that were connected to a reaction frame and to the loading beam. Two displacement cable transducers (C1 and C2) were placed at the ends of the loading beam to monitor axial displacements of the columns and rotation of the loading beam. In addition, either three or four strain gauges (SGs) were used to measure the strains of the light gauge steel section at mid-length of the columns. The strain gauges recorded an average peak longitudinal strain of 0.073%, corresponding to an average stress of 148 MPa. This average stress is in close agreement with the average stress capacity of the light gauge steel section of the steel-only stub columns (140 MPa). This consistency in results is due to the strains gauges

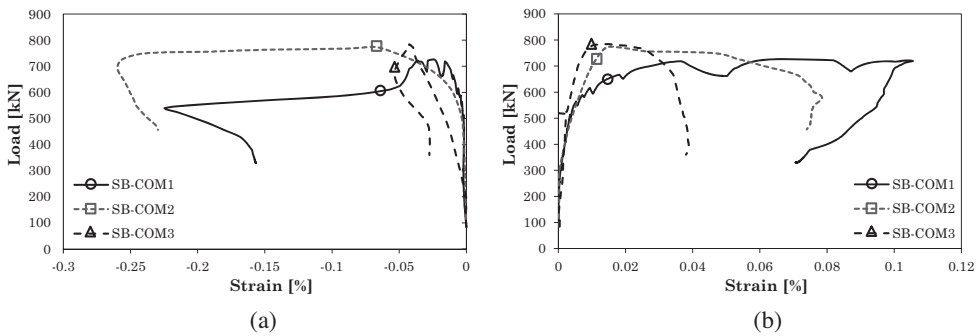

Fig. 14. Average strain on steel section at mid-height of composite columns: (a) longitudinal strain on front face; and (b) lateral strain on back face.

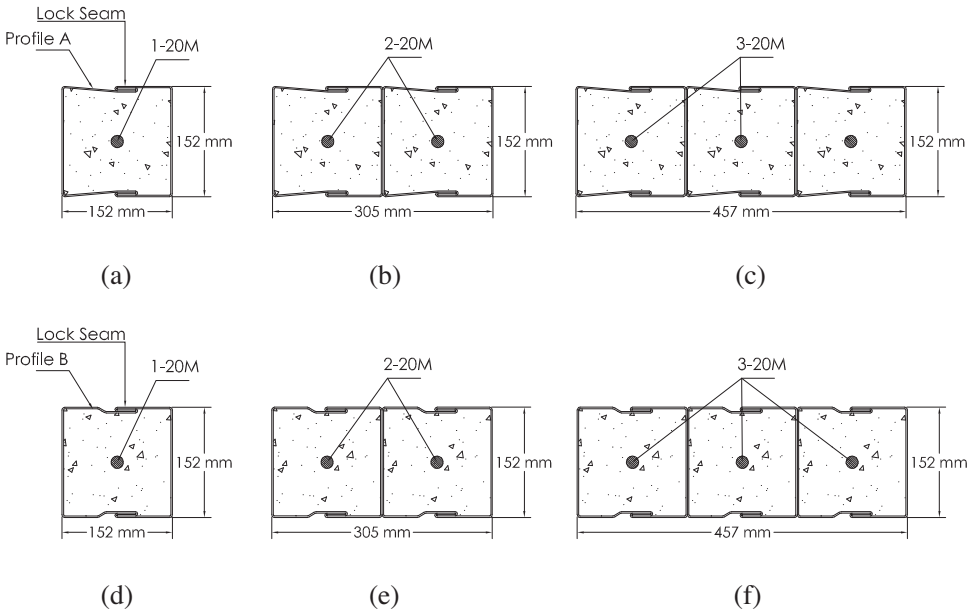

Fig. 15. Column cross section: (a) Columns C6, Profile A; (b) Columns C12, Profile A; (c) Columns C18, Profile A; (d) Columns C6, Profile B; (e) Columns C12, Profile B; and (f) Columns C18, Profile B.

Table 4
Details of long columns.

Column	Cross-Section	Length	Concrete Core	Encasing Steel	
	(mm × mm)	(mm)	f'_c (MPa)	f_y (MPa)	E_s (MPa)
C6-A8-1	152 × 152	2440	34	429	204,000
C6-A8-2	152 × 152	2440	34	429	204,000
C6-A9	152 × 152	2745	34	429	204,000
C6-B9	152 × 152	2745	34	429	204,000
C12-A8	152 × 305	2440	34	429	204,000
C12-A9	152 × 305	2745	34	429	204,000
C12-B8	152 × 305	2440	34	429	204,000
C12-B9	152 × 305	2745	34	429	204,000
C18-A8	152 × 457	2440	34	429	204,000
C18-A9	152 × 457	2745	34	429	204,000
C18-B8	152 × 457	2440	34	429	204,000
C18-B9	152 × 457	2745	34	429	204,000

Note: f'_c = cylinder compressive strength on day of test; f_y = yield strength; and E_s = modulus of elasticity

being located away from any influence of local buckling, and therefore, providing similar results to the global strains recorded for the stub columns.

Columns C6 were controlled by end bearing failure that involved crushing of the concrete and local buckling of the encasing light gauge steel and internal reinforcing steel (Fig. 17(a)). The C12 columns also experienced end bearing failure that involved crushing of the concrete, local buckling of the light gauge steel and internal steel, and separation of the two, 152 mm × 152 mm, modules that formed the cross section of the columns (Fig. 17(b)). Failure of the C18 columns was similar to the C12 columns, including separation of the three sectional modules (Fig. 17(c)). Separation of the three sectional modules was not observed for Column C18-B8. Due to twisting of the loading beam and the lack of actuator capacity to fail Column C18-B8, the test was halted and then repeated. The first and second tests were named C18-B8-1 and C18-B8-2, respectively.

The axial load capacity of the columns was proportional to the cross sectional area. This was a result of the load capacity being governed by end bearing, which is a sectional limit state and independent of column length. Columns C12 and C18 sustained an average load increase of 107% and 231% compared to Columns C6, respectively. The measured axial peak

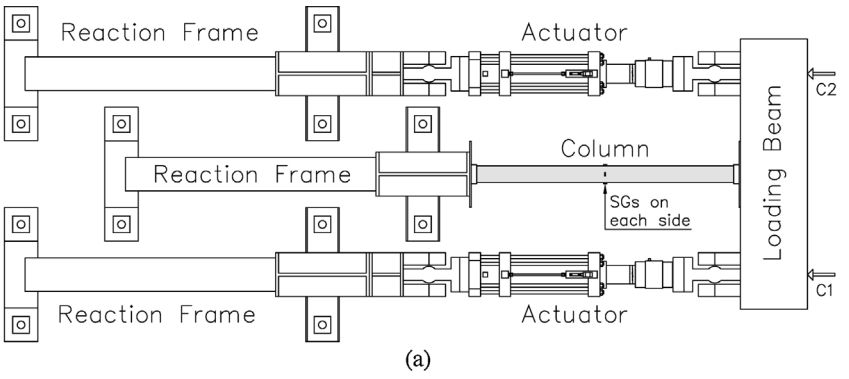

Fig. 16. Test setup: (a) schematic with two actuators with instrumentation (top view); (b) assembly with two actuators; and (b) assembly with three actuators.

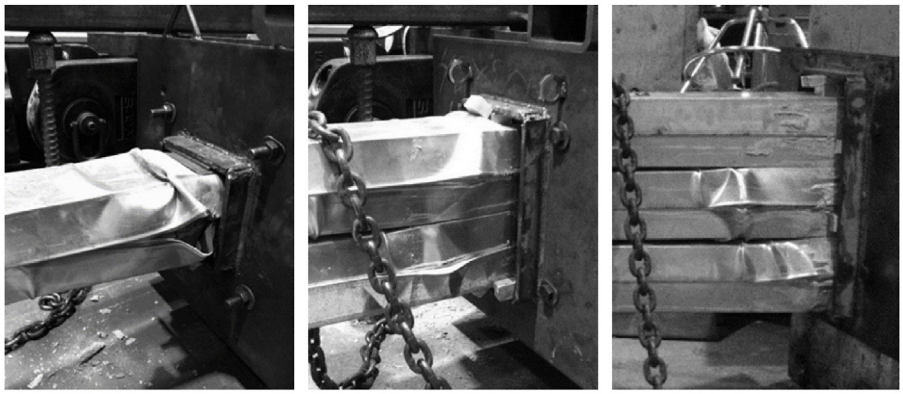

Fig. 17. Typical damage of columns: (a) Columns C6; (b) Columns C12; and (c) Columns C18.

strengths are reported in Table 5. Complete stress-strain responses are provided elsewhere [32]. Based on the properties of the columns, the effective moment of inertia (70% of the gross moment of inertia as specified by CAN/CSA-A23.3-14), and the pinned support condition, Euler's critical loads for Columns C6, C12, and C18 were 1308 kN, 2616 kN, and 3924 kN, respectively. None of the columns experienced loads that exceeded the calculated Euler's critical load; therefore, the long columns tested in this study were not governed by global buckling.

5. Calculated strength of full-scale columns

It was observed that all full-scale columns failed by end bearing. Given the length of the columns and failure mode, the effect of confinement of the encasing light gauge steel section was negligible and, therefore, not included in the calculation of

Table 5
Observed and predicted axial strength capacity of full-scale composite columns.

Column	Axial Strength [kN]				Calculated/Observed
	Observed	Calculated			
		Concrete	Steel Section (strain%)	Total	
C6-A8-1	745	628	136 (0.074%)	764	1.03
C6-A8-2	651	628	83 (0.045%)	711	1.09
C6-A9	847	628	184 (0.100%)	812	0.96
C6-B9	810	638	168 (0.091%)	806	1.00
C12-A8	1517	1255	254 (0.069%)	1509	1.00
C12-A9	1400	1255	243 (0.066%)	1498	1.07
C12-B8	1753	1277	355 (0.096%)	1632	0.93
C12-B9	1656	1277	214 (0.058%)	1491	0.90
C18-A8	2408	1883	459 (0.083%)	2342	0.97
C18-A9	2676	1883	216 (0.039%)	2099	0.78
C18-B8-1	1827	–	–	–	–
C18-B8-2	1820	–	–	–	–
C18-B9	2495	1915	432 (0.078%)	2347	0.94
AVERAGE					0.97
COV					8.7%

the concrete contribution. Furthermore, global lateral buckling of the columns was not observed at the peak compressive load capacity during testing. Therefore, the theoretical axial strength capacity of the columns was estimated from the sum of the concrete bearing resistance according to the requirements of the Canadian Standards Association Standard A23.3-14 for Design of Concrete Structures [33] (Eq. (4)) and the contribution of the light gauge steel, based on the average strain measured by the strain gauges (see Table 5) located at the mid-length of the columns at the peak recorded axial load (Eq. (5)).

$$N_c = 0.85 A_c f'_c \tag{4}$$

$$N_s = A_s E_s \varepsilon_s \tag{5}$$

Where A_c is the cross-sectional area of the concrete core, f'_c is the compressive strength of concrete (34 MPa), A_s is the cross-sectional area of the light gauge steel, E_s is the modulus of elasticity of the light gauge steel (204 GPa), and ε_s is the average strain of the light gauge steel measured at peak load during testing.

The internal steel reinforcing bars were well within the elastic range (according to the recorded strains at failure) and were not sufficiently developed in the concrete at the ends of the columns. Therefore, contribution of the internal reinforcing steel was not included in the predictions. In addition, calculations for Columns C18-B8-1 and C18-B8-1 were omitted due to challenges encountered during testing. In general, the calculated axial strength capacities based on the combined contribution of the concrete core and light gauge steel were conservative and in close agreement with the measured strengths (Table 5), with the exception of Columns C6-A8-1, C6-A8-2 and C12-A9. The calculated strength for Column C6-A8-1 was only 3% larger than the measured strength, which lies within an acceptable range of overestimation. Columns C6-A8-2 and C12-A9 are anomalies; their recorded axial strength capacities were significantly lower than the columns in their group (Table 5). It is probable that these discrepancies were due to out-of-plane deformations, which were not recorded during testing, affecting the strains measured by the strain gauges and the stresses sustained by the steel sections. In addition, the full cross sectional area of the steel sections, including the lock seams, were used in the calculation of the steel contribution. It is probable that the entire steel section was not loaded uniformly during testing. [Note that the cross sectional area with lock seams is approximately 20% larger than the nominal area.] Furthermore, a very conservative strength was calculated for Column C18-A9. Low prediction for this column may be attributed to the low strain used in the calculations, which was based on a single strain gauge that was not representative of the average strain of the steel section.

Based on the limited test data presented herein and not considering the anomalous columns noted above (C6-A8-2, C12-A9, and C18-A9), the axial compressive strength resistance of the light gauge steel composite columns was calculated using the proposed Eq. (6), where the contribution of the steel section, N_s, is calculated assuming an upper limit on the stress for the steel section. The limit ($1/3 f_y$) is based on the results from the steel-only stub columns (140 MPa). This stress limit is in close agreement with the effective stress of 137 MPa, which was calculated using the North American Specification for the

Design of Cold Formed Steel Structural Members (CSA S136-07) for slender webs with slender parameter λ greater than λ_c (Class 4 sections). The effective stress is based on the critical stress for stiffened elements supported by a web on each longitudinal edge, determined with the plate buckling coefficient of 4 and the properties of the steel sections.

$$N_s = (1/3) f_y A_s \tag{6}$$

Comparison of the predicted (summation of Eqs. (4) and (6)) and the observed axial strength of the full-scale composite columns (Fig. 18) suggests that Eq. (6) provides a conservative contribution of the steel section. The average predicted-to-observed ratio is 0.94, and the corresponding standard deviation is 5.1%. These predictions are preliminary and require further testing to validate the proposed contribution of light gauge encasing steel and to explicitly determine the contribution of the concrete core to restraining local buckling of the steel section.

6. Conclusions

The compressive strength capacity of concrete-filled light gauge steel composite columns was experimentally determined in this study by testing fourteen stub columns and twelve full-scale columns. Results from the stub columns were used to assess the effect of confinement, local buckling, and individual contributions of the components to the axial capacity of the full-scale light gauge composite columns. The findings of this study are applicable to width-to-thickness ratio of the encasing steel section of 125. Further experimental studies are required to corroborate these findings for other width-to-thickness ratios.

Two parameters were investigated in the stub column tests: concrete contribution including effect of confinement, and encasing steel contribution including local buckling. The test results demonstrated that the concrete strength was increased by approximately 16% due to the effect of confinement. The observed effect of confinement applied only to the stub columns that consisted of shorter encasing steel sections that were not subject to axial loading. The gain in strength due to confinement was negligible for the full-scale columns, where failure was localized at the ends of the columns (end bearing failure). Therefore, the beneficial effect of confinement should not be included in evaluating the strength of full-scale columns encased by light gauge steel. Results from the steel-only stub columns illustrated that local buckling controlled the strength of the steel sections when not restrained by the concrete core. The observed average strength capacity of the steel section was 33% of the tensile capacity of the section.

The load capacity of the full-scale composite columns was proportional to the cross sectional area. Columns C12 and C18 sustained approximately double and triple the load of Columns C6. The compressive capacity of the full-scale columns was controlled by end bearing, which is a cross sectional limit state independent of length.

The axial strength capacity of the concrete-filled light gauge steel full-scale columns was estimated with end bearing resistance as the limit state according to CSA A23.3-14 and the average strain of the light gauge steel section at mid-length. The calculations did not include any contribution from the internal steel reinforcing bars. The calculated strength capacities were in good agreement with those recorded. The calculated-to-recorded strength was 0.97. In addition, a preliminary limit on the contribution of the steel section of 33% of the yield capacity as observed with the steel-only stub columns was suggested. The predicted-to-recorded strength ratio was 0.94. The limit on the steel contribution provided satisfactory results; however, further testing and validation are required.

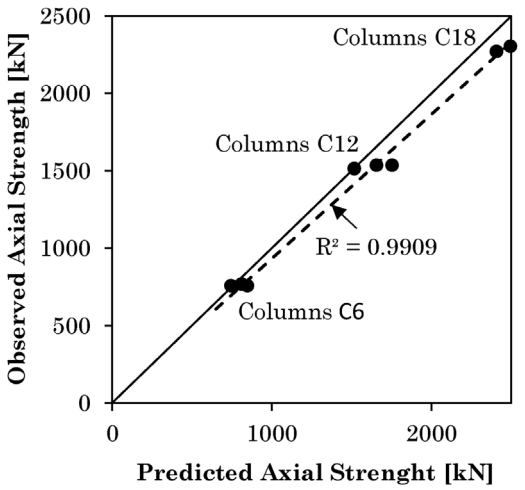

Fig. 18. Comparison of predicted and observed axial strength capacity.

Acknowledgments

The authors would like to express their gratitude to the Natural Sciences and Engineering Research Council for providing financial assistance through the Engage Grants Program [grant number EGP 428565-11]. The donation of materials from B.J. Normand Ltd. is gratefully acknowledged.

References

[1] MUR-TEC Systems Inc. MUR-TEC Systems Inc.: An Innovative Way of Building, Ottawa, Ontario (2009).
[2] ACI Committee 318. Building code requirements for structural concrete and commentary, ACI 318–14, American Concrete Institute, Farmington Hills, Michigan (2014).
[3] AIJ. Recommendations for design and construction of concrete filled steel tubular structures, Architectural Institute of Japan, Tokyo (2008).
[4] Standards Australia. Bridge design – Steel and composite construction, AS5100 Part 6, Standards Australia, Sydney (2004).
[5] BSI. Steel, concrete and composite bridges, BS5400, Part 5: Code of practice for design of composite bridges, British Standards Institute, London (2005).
[6] CSA. Limit States Design of Steel Structures, CSA S16–14, Canadian Standards Association, Mississauga, Ontario (2014).
[7] DBJ13-51. Technical specification for concrete-filled steel tubular structures, The Construction Department of Fujian Province, Fuzhou (2003).
[8] Eurocode 4. Design of composite steel and concrete structures, Part 1.1: General rules and rules for buildings, EN1994–1-1:2004, European Committee for Standardization, Brussels (2004).
[9] H. Shakir-Khalil, M. Mouli, Further tests on concrete-filled rectangular hollow-section columns, Struct. Eng. 68 (20) (1990) 405–413.
[10] S.P. Schneider, Axially loaded concrete-filled steel tubes, J. Struct. Eng. ASCE 124 (10) (1998) 1125–1138.
[11] K. Sakino, H. Nakahara, S. Morino, I. Nishiyama, Behavior of centrally loaded concrete-filled steel-tube short columns, J. Struct. Eng. ASCE 130 (2) (2004) 180–188.
[12] H.B. Ge, T. Usami, Strength of concrete-filled thin-walled steel box columns: experiments, J. Struct. Eng. ASCE 118 (11) (1992) 3036–3054.
[13] Y.F. Yang, L.H. Han, Concrete filled steel tube (CFST) columns subjected to concentrically partial compression, Thin-Wall. Struct. 50 (1) (2012) 147–156.
[14] Q.X. Ren, L.H. Han, D. Lam, C. Hou, Experiments on special-shaped CFST stub columns under axial compression, J. Constr. Steel Res. 98 (2014) 123–133.
[15] F. Zhou, B. Young, Numerical analysis and design of concrete-filled aluminum circular hollow section columns, Thin-Wall. Struct. 50 (1) (2012) 45–55.
[16] S. El-Tawil, G.G. Deierlein, Strength and ductility of concrete encased composite columns, J. Struct. Eng. ASCE 125 (9) (1999) 1009–1019.
[17] B. Lakshmi, N.E. Shanmugam, Nonlinear analysis of in-filled steel-concrete composite columns, J. Struct. Eng. ASCE 128 (7) (2002) 922–933.
[18] B. Uy, Strength of concrete-filled steel box columns incorporating local buckling, J. Struct. Eng. ASCE 126 (3) (2000) 341–352.
[19] Q.Q. Liang, B. Uy, Theoretical study on the post-local buckling of steel plates in concrete-rolled box columns, Comput. Struct. 75 (2000) 479–490.
[20] Q.Q. Liang, B. Uy, J.Y.R. Liew, Strength of concrete-Filled steel box columns with local buckling effects, in: M. Stewart, B. Dockrill (Eds.), Proceedings of the Australian Structural Engineering Conference 2005: Structural Engineering and Building into the Future, Newcastle, Australia, 2005, pp. 1104–1113.
[21] C.C. Chen, J.W. Ko, G.L. Huang, Y.M. Chang, Local buckling and concrete confinement of concrete-filled box columns under axial load, J. Constr. Steel Res. 78 (2012) 8–21.
[22] Z. Tao, Z.B. Wang, Q. Yu, Finite element modelling of concrete-filled steel stub columns under axial compression, J. Constr. Steel Res. 89 (2013) 121–131.
[23] H. Thai, B. Uy, M. Khan, Z. Tao, F. Mashiri, Numerical modelling of concrete-filled steel box columns incorporating high strength materials, J. Constr. Steel Res. 102 (2014) 256–265.
[24] X. Dai, D. Lam, Axial compressive behaviour of stub concrete-filled columns with elliptical stainless steel hollow sections, Steel Compos. Struct. 10 (6) (2010) 517–539.
[25] N. Ferhoune, Experimental behaviour of cold-formed steel welded tube filled with concrete made of crushed crystallized slag subjected to eccentric load, Thin-Wall. Struct. 80 (2014) 159–166.
[26] N. Ferhoune, J. Zeghiche, Experimental behaviour of concrete-filled rectangular thin welded steel stubs (compression load case), C.R. Mec. 340 (2012) 156–164.
[27] E. Ellobody, B. Young, Design and behaviour of concrete-filled cold-formed stainless steel tube columns, Eng. Struct. 28 (2006) 716–728.
[28] D. Lam, L. Gardner, Structural design of stainless steel concrete filled columns, J. Constr. Steel Res. 64 (2008) 1275–1282.
[29] J.E. Lundberg, The reliability of composite columns and beam columns. Struct Eng Rep No. 93-2 1993, Department of Civil and Mineral Engineering, University of Minnesota, Minneapolis, Minnesota.
[30] CSA. North American specifications for the design of cold-formed steel structural members, CSA S136-12, Canadian Standards Association, Mississauga, Ontario (2012).
[31] Y. Yang, C. Hou, Z. Wen, L. Han, Experimental behaviour of square CFST under local bearing forces, Thin-Wall. Struc. 74 (2014) 166–183.
[32] W.L. Cortés-Puentes, A. Abdulridha, M. Majeed, D. Palermo, B. Normand, Performance of concrete-filled light gauge steel composite columns: pilot study, Proceedings of the 3rd Specialty Conference on Material Engineering and Applied Mechanics, Montreal, Canada, 29 May–1 June, 2013 (paper MEC-45).
[33] CSA. Design of Concrete Structures, CAN/CSA-A23. 3–14, Canadian Standards Association, Mississauga, Ontario (2014).